Evaluation of mass measurement techniques for soot with different size distributions and OC/TC contents

Benoît Sagot[1], Guillaume Pailloux[2], Amel Kort[2]

[1] ESTACA, ESTACA'Lab - Paris Saclay, Montigny-Le-Bretonneux, F-78180, France
[2]Autorité de Sûreté Nucléaire et de Radioprotection (ASNR), PSN-RES/SCA/LPMA, F-91400, Saclay, France

Correspondence to: Benoît Sagot (Benoit.sagot@estaca.fr)

Abstract. This study focuses on measuring mass concentration of soot aggregates generated with a Mini-CAST burner. The experiments were performed in a test bench able to generate soot particles with different size distributions and different OC/TC ratios. With this soot production, we assessed the mass concentration measurements based on four online instruments (TEOM, PPS, MA300 and SMPS) and an offline gravimetric measurement. The OC/TC ratio was also determined. The findings demonstrate that the TEOM measurements were performed within acceptable limits of 10 % in comparison to the gravimetric measurements, over a wide range of OC/TC ratio, mass concentration and size distribution. The TEOM measurements were therefore considered as the reference. The Pegasor Particle Sizer (PPS) mass concentration measurement which is based on the aerosol electrical charging is calibrated for a reference size distribution, and we suggested a correction of the mass concentration measurement based on the aerosol Fuchs active surface, that proved to be efficient within the limits of this study. Finally, we confirmed that the mass concentration measurements obtained with the MA300 aethalometer are OC/TC ratio and wavelength dependent, and we were able to establish OC/TC limits for the overall mass concentration evaluation with the infrared and ultraviolet wavelengths.

1 Introduction

In the context of studies on airborne dispersion of soot particles emitted during fire scenarios and monitoring and quantification of emissions from thermal engine, it is important to have a robust measurement of the mass concentration of emitted soot. These measurements are needed to assess the consequences of fires in Basic Nuclear Installations (Kort et al., 2022), as soot is responsible for clogging the last containment barrier made by HEPA filters, or for the metrology of conventional engines PM emissions (Aakko-Saksa et al., 2022). Dynamic real-time monitoring of mass emissions can be performed using various types of instruments based on different measurement principles, such as the real-time aethalometer-type measurement (MA300), the Tapered Element Oscillating Microbalances (TEOM) or the Pegasor Particle Sensor (PPS). These instruments allow the study of aerosols across a wide range of concentrations, from ambient air quality monitoring to highly concentrated exhaust emissions. The quantification performed by the PPS is based on the electrical charge on the surface of aerosols, making it extremely dynamic. However, it requires calibration that primarily depends on the median diameter of the aerosol particle

size distribution. Similarly, the aethalometer is an instrument based on optical transmission through a soot cake collected on a filter, and its mass quantification is influenced by the physical nature of the soot, particularly the elemental carbon to organic carbon ratio. For time stable emission sources, it is also possible to perform measurements using filter sampling, which allows mass concentration quantification by weighing (gravimetric measurement) and OC/TC ratio (Organic Carbon to Total Carbon) determination using a Sunset Laboratory analyser. All these mass concentration measurement techniques, usually used in different contexts, need to be qualified in an intercomparison to provide reliable and robust measurements.

For this purpose, soot was generated by a mini-CAST JING 5201C burner through the combustion of propane. Different studies have demonstrated that this mini-CAST generator can produce soot with a wide range of sizes and properties and is considered as a relevant tool to produce soot similar to those emitted by different combustion processes such as aircraft engine (Marhaba et al., 2019) or fire situation (Kort et al., 2021). It has been extensively used for soot characterization and as a time stable soot production source: by varying the gas flow rates supplied to this generator, it is possible to adjust the mass concentration over a wide range, as well as the particle size distribution and the elemental carbon to organic carbon ratio of the produced soot particles. The concentrations of soot generated are then either collected on a filter for ex-situ measurements or diluted using a double stage ejector-type diluter Dekati E-diluter, which delivers concentrations compatible with the measurement ranges of the instruments used.

The mass concentration evaluated by the online devices (MA300, PPS Pegasor, SMPS) and the offline direct gravimetric measurement were studied as a function of the reference mass concentration evaluated by the TEOM. The evaluation of the OC/TC ratio done from the filters and the size distributions of the produced soot particles are also necessary for the interpretation of the instrument responses.

2 Experimental setup

For this experimental study, we developed a test bench (Fig. 1) dedicated to the mass concentration intercomparison. This setup includes the soot generation source, the mini-CAST, followed by two lines. One line, maintained at 180°C, is used for filter sampling, while the other feeds a dilution system that distributes the diluted and cooled aerosol to various measurement instruments: the TEOM, PPS, MA300, and SMPS. The sampling system was designed and operated in accordance with ISO 8178 requirements, which specify standardized procedures for measuring exhaust emissions from internal combustion engines. The following sections detail the operating principles and implementation conditions of each component of this test setup.

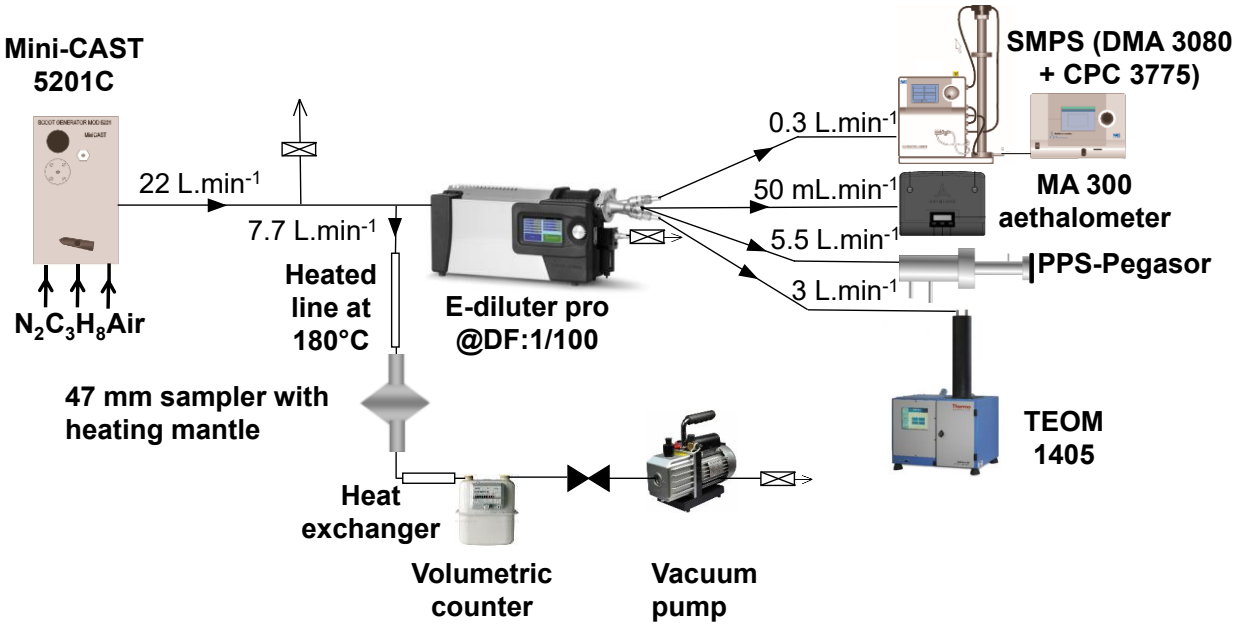

Figure 1 – Configuration of the experimental bench for intercomparison of mass concentration measurements

The aerosol source is a Mini-CAST 5201C soot generator, which produces polydisperse soot particles by propane combustion. The principle of soot generation by the Mini-CAST involves an axial laminar diffusion flame, which is quenched by a cold, dry nitrogen flow to stop the combustion process and prevent soot oxidation. A rapid dilution with clean, dry air reduces the soot concentration, thereby limiting particle coagulation. By varying the flow rates of fuel, oxidizing air, and mixing nitrogen, it is possible to modify the characteristics of the flame, particularly its temperature, which affects both the quantity and the properties of the produced soot particles (Moore et al., 2014). As in the study by Marhaba et al. (Marhaba et al., 2019), propane flow is maintained at 60 mL/min, nitrogen flow at 0 mL/min, dilution air flow at 20 L/min and quenching nitrogen flow at 7 L/min. Variations of the soot production were obtained by varying the oxidation air flow rate from 0.9 L/min up to 1.5 L/min (0.9, 1, 1.15, 1.2, 1.25, 1.3, 1.35 and 1.5 L/min). The measurement points with oxidation air flow rate at 1, 1.15 and 1.5 L/min correspond respectively to the CAST3, CAST2 and CAST1 operating points in the study of Marhaba et al. (Marhaba et al., 2019). These specific operating points were also chosen for different studies (Bescond et al., 2016; Ouf et al., 2016). During the tests, stable generation points were sought, and before initiating filter sampling, the stability of the concentration production was ensured through measurements taken with online instruments such as the PPS and TEOM. Each measurement point was repeated three times, and the error bars represent the standard deviation of these measurements.

A flexible heated line (1 m long with 6 mm internal diameter) connects the mini-CAST soot generator to the filter sampler, and is maintained at 180°C. This line is dedicated to sampling on quartz fiber filters (Whatman quartz filter, Grade QM-H, diam. 47 mm), for ex-situ gravimetric measurements, and for later OC/TC analysis. These filters are used for mass

quantification of soot concentration during stable generation conditions. Quartz filters are preconditioned by heating at 180°C in an oven for one hour to eliminate moisture. They are then weighed and stored with desiccant to prevent reabsorption of humidity. During measurements, the filters are placed in the 47 mm sampler with a 180°C temperature regulated heating jacket surrounding it. The collected mass is determined using a precision balance (Kern ABT 100-5M). The volume of gas passing through the filter is measured using a Gallus gas volumetric counter (see Fig. 1). Between the mass sampler and this Gallus volumetric counter, a heat exchanger cools the gas down to the ambient temperature, maintained at 20°C in the laboratory. By combining the collected mass with the measured gas volume, the soot mass concentration is calculated. This measurement is referred to as "Gravimetric mass concentration" in the study.

The Sunset Lab OC/EC field instrument (Sunset Laboratory) has been used for the measurement of the OC/TC ratio. Filters were analyzed based on the IMPROVE_A thermal protocol (Chow et al., 2001). In this instrument, to separate the organic fraction of carbon (OC) from the elemental fraction (EC), the samples are subjected to various temperature plateaus (up to 850°C) in a helium inert atmosphere for the OC fraction and in an oxidizing atmosphere for the EC fraction. The gases formed are then transported by the helium flow to a catalytic furnace, where they are oxidized to CO_2, then reduced to CH_4 for more accurate measurement by a calibrated Flame-Ionization Detector (FID). A thermo-optical correction is applied to separate OC from EC. OC/TC measurements have been performed on quartz fiber filters. Three punches of 1.5 cm^2 were analysed for each sample.

The second sampling line, after dilution, feeds real-time measurement instruments. The Dekati E-dilutor pro dilution system enables 2-stage dilution with a dilution factor set at 100. The first dilution stage is heated, while the second dilution stage operates at room temperature, where the aerosol sample is also cooled in a controlled manner. Both dilution stages are ejector-type, with a complementary sweep air flow in the duct. Concentrations downstream of the dilution system are compatible with the measurement ranges of the instruments used: a TEOM for a robust measurement of mass concentration, a PPS-Pegasor and a MA300 Aethalometer for real time mass concentration measurement and a SMPS for measurement of particle size distribution. The SMPS is composed of a Differential Mobility Analyzer (DMA 3080, TSI), which provides a mobility diameter size selection of particles, and a condensation particle counter (CNC 3775, TSI).

The TEOM (Thermo Scientific 1405) can continuously measure the mass of PM accumulating on a filter mounted upon an inertial microbalance using tapered element oscillating at its natural frequency (at 200 Hz). Aerosol is drawn in by a pump connected to the base of the microbalance. Sampled particles retained by the filter increase the mass of the oscillating system, producing a decrease in the natural frequency of vibration. Changes in the frequency of oscillation which are related to the mass of material accumulating on the filter are detected in quasi-real-time and converted by a microprocessor into an equivalent PM mass concentration (Allen et al., 1997). The sampled particles are heated at a temperature of 50°C.

The PPS is a real time sensor that can be used to provide the mass and number concentration of aerosols in the exhaust of car engine based on electrical measurement. The device is supplied with clean, dry compressed air. In the first phase, the clean air is ionized by the corona effect and ejected through an orifice (Ntziachristos et al., 2013). Particles are electrically charged by the binding of ions within a zone isolated by a Faraday cage. Only the small number of ions that charge the particles surface

are lost to the sensor outlet where an electrometer is used to measure the "compensation" electrical current. It is related to the particle number concentration and particle size, and Ntziachristos et al. (2004) demonstrated that this instrument provides a measure of the active surface area of the studied aerosol (Rostedt et al., 2014).

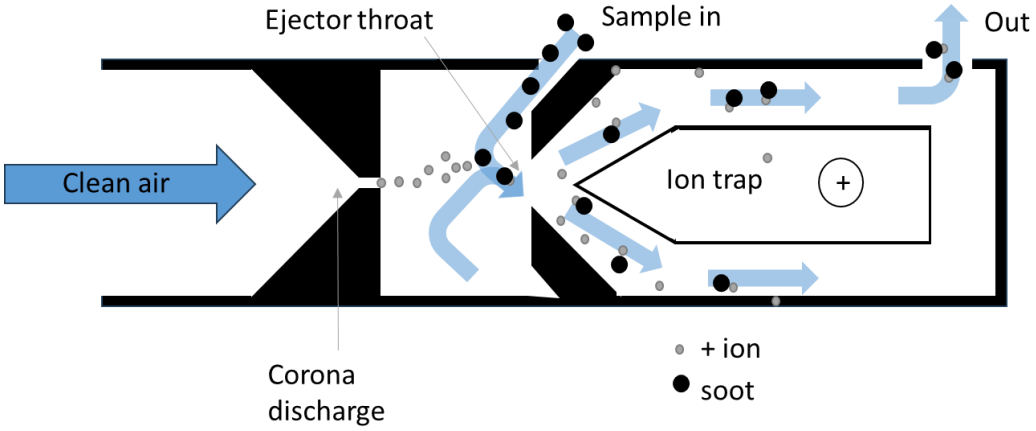

Figure 2 – PPS operating principle

The raw current measurement is then used to determine the mass or number concentrations of sampled particles using calibration coefficients dependent on particle size. The remaining free ions with a high electrical mobility are eliminated by an ion trap. In addition, the injector design protects the corona needle, and the charged particles are sensed with no need for contact with the sensor which can be beneficial in these polluted environments (Maricq, 2013). Despite the PPS ability to track emissions dynamically (at Hz frequency) under high number and mass concentrations that can be useful for real-time emission monitoring in fire situations, the PPS mass calibration factor was established essentially on automobile emissions with a relatively limited range of size distribution in number (Ntziachristos et al., 2013) and OC/TC ratios which were not indicated in their study.

The MA300 aethalometer (AethLabs, San Francisco) is a real time portable analyzer that uses the filter-based light absorption principle: the mass concentration measurement is based on the optical attenuation ATN of a light beam passing through a cake of particles collected on a filtering fiber tape. The instrument has five analytical channels that operate at different wavelengths (375, 470, 528, 625 and 880 nm), and the measurement of absorption at 880 nm is interpreted as Black Carbon (Hansen et al., 1984). The MA300 draws a controlled flow through the collection spot on the filter tape, and when the light attenuation reaches a threshold value, the tape advances automatically.

The attenuation ATN is defined (Gundel et al., 1984) as $ATN = -100 * \ln(I/I_0)$, with I and I_0 respectively the measured intensity trough the loaded spot signal and the reference signal, through the empty filter (see Fig. 3). The instrument measures the transmission of light through the particle-loaded filter, from which the attenuation (ATN) is derived based on its rate of change over time. This attenuation is then converted into an absorption coefficient. Finally, the equivalent black carbon mass concentration is obtained by dividing the absorption coefficient by σ_{MAC}, the Mass Absorption Coefficient (MAC) specific to

black carbon (Drinovec et al., 2015). With this definition and for the 880 nm wavelength, the deposited equivalent Black Carbon eBC mass concentration is then evaluated as:

$$eBC = \frac{S \cdot (\Delta ATN/100)}{Q \cdot \sigma_{MAC} \cdot C_{ref} \cdot (1 - k \cdot ATN) \cdot \Delta t} \quad (1)$$

where S is the collection spot area, ΔATN the changes of attenuation during interval Δt, Q the measured flow rate after accounting for the instrument internal leakage, Δt the time interval between two measurements, C_{ref} the multiple scattering correction factor, k a compensation parameter for filter loading effect correction. Since the airflow is measured downstream of the filter, potential leakage may occur and should be accounted for. However, recent studies using MA300 and MA350 aethalometers (Chakraborty et al., 2023; Elomaa et al., 2025) considered these leakage as negligeable, as we did in this study. The filter-based light absorption techniques are subject to measurement artifacts due to scattering on the filter (Weingartner et al., 2003). These empirical parameters are related to the instrument design and filter material (Wu et al., 2024). The C_{ref} parameter considers multiple scattering correction factor, which mainly depends on the properties of the filter substrate, and on the optical characteristics of the aerosol deposited on the filter, with no significant spectral dependence (Drinovec et al., 2015). For the MA300 aethalometer, the sampling filter tape is composed of PTFE (polytetrafluoroethylene), and the manufacturer calibrated a value of C_{ref} = 1.3. The mass absorption coefficient σ_{MAC} at 880 nm wavelength is $\sigma_{MAC} = \sigma_{ATN} / C_{ref} = 10.12/1.3 = 7.8\ m^2.g^{-1}$. The Specific Attenuation Cross-section σ_{ATN} is wavelength-dependent and was taken from the instrument manufacturer's specifications, with values ranging from σ_{ATN} =10.12 $m^2.g^{-1}$ for IR at λ=880 nm, up to σ_{ATN} =24.069 $m^2.g^{-1}$ for UV at λ=375 nm. The fixed MAC values used in aethalometers may not accurately represent the true MAC of the sampled soot aerosol, as MAC can vary with aerosol composition (Chakraborty et al., 2023), including the OC/TC ratio, thus introducing uncertainty in the reported eBC concentrations. Sipkens et al. (2025) cite several mechanisms that can explain the variability of MAC between aerosol samples, including intraparticle scattering (the "lensing effect"), the condensation of semi-volatile materials on soot, and variations in particle size. This recent study evaluated operational uncertainties through an inter-comparison of five aethalometers. The results showed that these uncertainties scale with mass concentration, with inter-device multiplicative errors of around 10 % under favorable conditions (Sipkens et al., 2025), such as extended measurement periods or high aerosol loadings. One of the identified drawbacks of aethalometers is the overestimation of BC concentration on a new filter and the underestimation when the loading is high, with the most accurate concentrations being obtained on slightly loaded filters (Arnott et al., 2005; Collaud Coen et al., 2010). Several models have been proposed to correct this loading effect when processing aethalometers data, such as Weingartner et al. (2003) and Virkkula et al. (2007) models, which have been most frequently used for loading effect compensation. Drinovec et al. (2015) developed a real-time method to compensate nonlinearity with high time resolution, by using a double collection on two spots in parallel at different flow rates. In this method, the k constant is evaluated for each wavelength, and this so-called "dual-spot technology" permits to eliminate the data artifact due to filter loading. In this study, the MA300 aethalometer employs the dual-spot technology to eliminate data distortions caused by filter loading. The sensor applies a variant of the dual-spot correction (Chakraborty et al., 2023; Mendoza et al., 2024), with the parameter k evaluated using Equation (2)

$$k = \frac{eBC_L - eBC_H}{(eBC_L \times ATN_H) - (eBC_H \times ATN_L)} \quad (2)$$

Where L and H stand respectively for the low and high flowrates used in this dual-spot technology.

Aethalometers have been used to monitor black carbon concentrations in urban areas (Blanco-Donado et al., 2022), assess biomass burning contribution to emissions in urban areas (Favez et al., 2007), or to measure personal exposure in working environment (Gren et al., 2022). However, the ability of aethalometers to accurately quantify soot emissions remains an active research topic. The recent study by Aakko-Saksa et al. (2022) over a wide ship exhaust test matrix obtained with different fuels, engines, and emission control devices showed that measurement with an aethalometer could lead to overestimation of BC emissions.

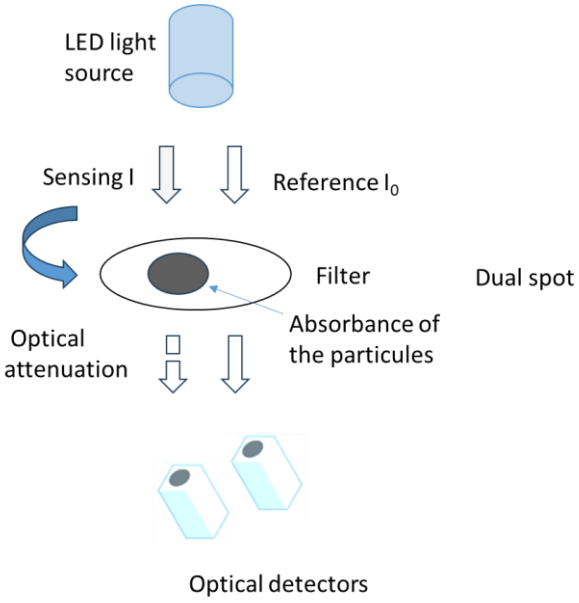

Figure 3 – MA300 operating principle

Results and discussion

Fig. 4 shows the evolution of the reference (TEOM) mass concentration (left) and the number size distribution measured by the SMPS (right) as a function of oxidation air. When changing the oxidation air flow rate, the main parameter that vary is the fuel–air equivalence ratio Φ, describing the flame in terms of fuel-lean (Φ < 1), stoichiometric (Φ = 1), and fuel-rich (Φ >1) conditions (Marhaba et al., 2019).

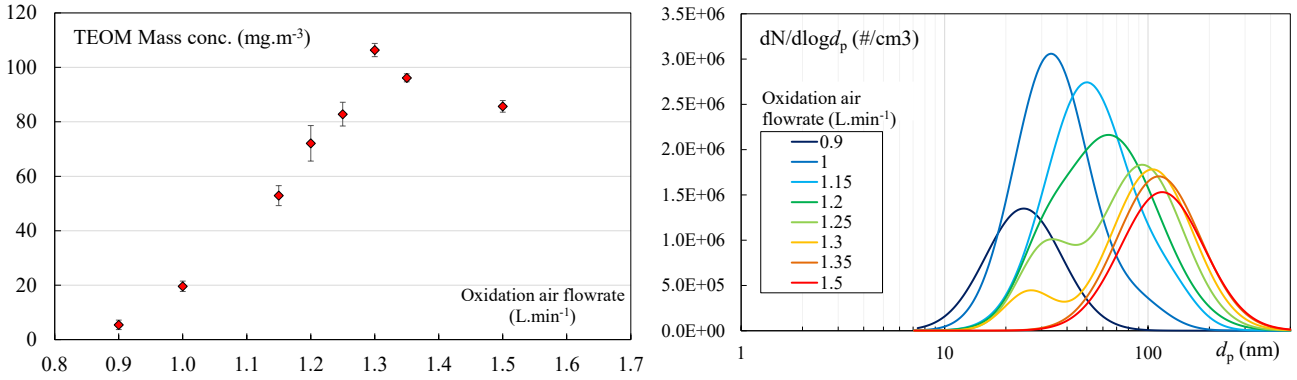

Figure 4 – Evolution of the reference (TEOM) mass concentration (left) and the number size distribution (right) as a function of oxidation air

For oxidation air of 0.9 L.min^{-1}, the size distribution of generated soot particles is monomodal with a number median diameter of 23.3 nm and the lowest mass concentration of 5.44 mg.m^{-3}. Moore et al. (Moore et al., 2014) showed that by continuously increasing the oxidation air flowrate, the volumetric soot production reaches a maximum at a value close to 1.3 L/min when the adiabatic temperature of the flame reaches its maximum, with a strong impact on the OC/TC organic-to-total carbon ratio. In our experiments, intermediate values of the oxidation air were thus added. When increasing the oxidation air flowrate, the produced mass concentration increases up to a maximum of 106.39 mg.m^{-3} for soot generated corresponding to an oxidation air flowrate of 1.3 L.min^{-1}. For this generation point, a bimodal size distribution is obtained. For higher oxidation airs, a decrease of the mass concentration is then observed. When reaching 1.5 L.min^{-1}, the size distribution becomes monomodal again with the highest modal median diameter of 113.4 nm and a mass concentration of 85.68 mg.m^{-3}. The measured particle size distributions were fitted with the sum of two log normal distributions that correspond to an ultrafine and a fine mode. We describe in Table 1 the nature of the distribution, and report, for each operating point, the median diameters of the two modes as well as their respective intensities expressed as a percentage. We also indicate the number median diameter of the measured distribution.

Table 1 – Main characteristics of the number size distributions for each of the operating points studied

Oxidation air (L.min^{-1})	Nature of the distribution	Mode 1 (nm)	Mode 2 (nm)	Number median diameter (nm)
0.9	monomodal	24.5 nm - 100%	(-)	23.3
1	bimodal	33.3 nm - 93%	90.5 nm - 7%	33.4
1.15	bimodal	49.9 nm - 92%	126.6 nm - 8%	51.4
1.2	bimodal	29.8 nm - 9%	64.7 nm - 91%	59.4
1.25	bimodal	31 nm - 25%	93.7 nm - 75%	73.7
1.3	bimodal	26 nm - 13%	105.2 nm - 87%	94.7
1.35	monomodal	(-)	113 nm - 100%	109.4

1.5	monomodal	(-)	117.3 nm - 100%	113.4

Fig. 5 shows a parity curve of the mass concentrations measured by the TEOM, as a function of the gravimetric reference measurements. Over a two decades wide mass concentration range, mass concentrations measured by the TEOM remain within a 10% interval of the gravimetric reference for all eight tested oxidation air flowrates (values indicated next to each data point, in $L \cdot min^{-1}$). Based on ISO 16450 we have evaluated the slope and offset of the orthogonal assessment. The linear regression established between the reference and tested measurements satisfies the ISO 16450 validation criteria, with the slope b statistically compatible with unity ($|b - 1| < 2u_b$), and the intercept a close to zero and statistically compatible with it ($|a| < 2u_a$), where u_b and u_a are the standard uncertainties associated with the slope and intercept, respectively. So, we have established the equivalence between the TEOM and the gravimetric measurement. Finally, we concluded that the TEOM should be considered as the reference measurement, being online in the exact same conditions downstream the dilution system. For this uncertainty evaluation, we followed ISO 15767 to assess the uncertainty related to weighing, evaluated the uncertainty on the sampled volume, and applied uncertainty propagation to estimate the overall uncertainty, which combines measurement uncertainty with the uncertainty associated with repeatability based on the three repetitions. The error bars shown in Figure 5 for the "Gravimetric mass conc." result from this analysis.

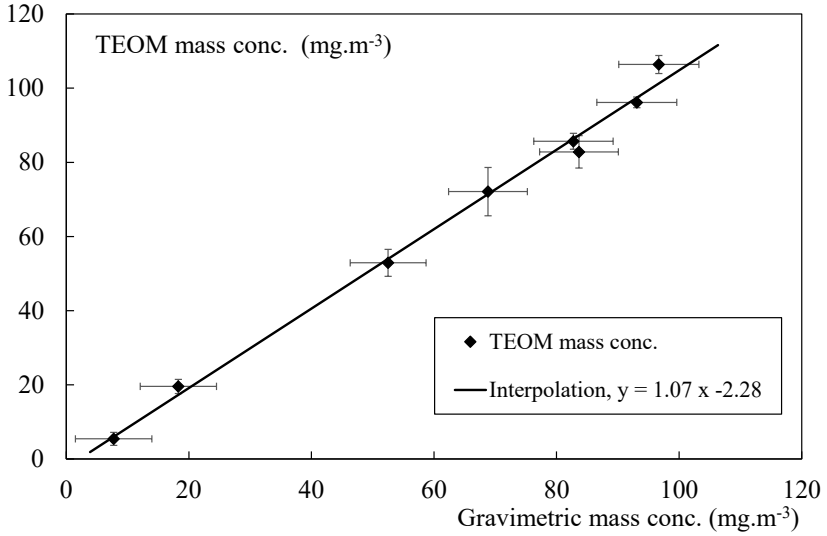

Figure 5 – Parity curve of measured TEOM mass concentrations as a function of the gravimetric reference measurements, with the corresponding interpolation.

Fig. 6 (left) shows the mass concentrations measured by the PPS, as a function of those measured by the TEOM for soot produced with the different oxidation air flow rates tested. Fig. 6 (right) shows the evolution of the mass concentration ratio measured by the PPS and by the TEOM as a function of the SMPS measured number median diameter. This ratio logically increases as the median diameter decreases. Indeed, the PPS estimates the particle mass based on their active surface area (Ntziachristos et al., 2004). For spherical particles with a constant diameter, the mass is proportional to the cube of the particle

diameter, while the surface area scales with the square of the diameter, resulting in a surface-to-mass ratio that varies as 1/Diameter. With the calibration performed on a polydisperse soot aerosol produced by an engine, the mass is correctly estimated for median diameters close to 80 nm.

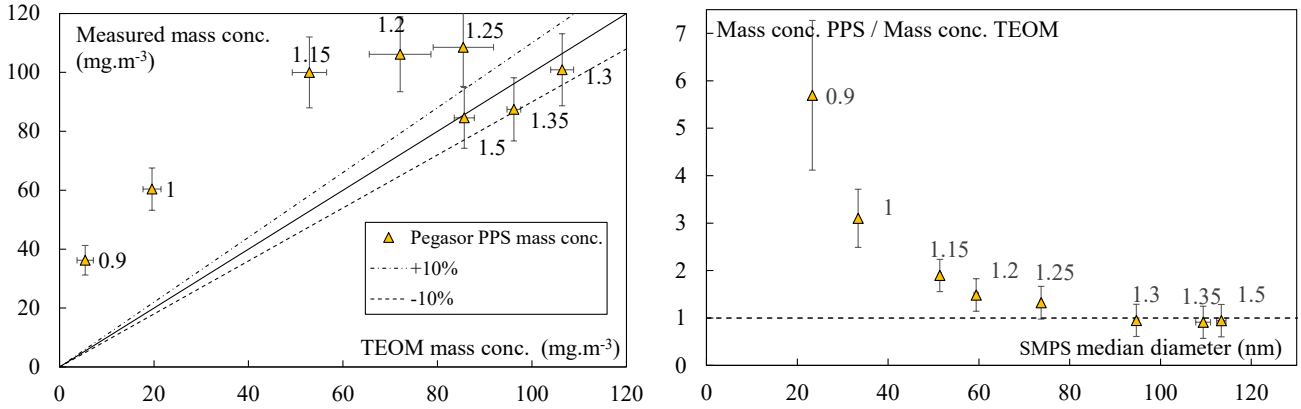

Figure 6 –Mass concentrations measured by the PPS-Pegasor as a function of the TEOM reference measurements (left) and ratio of mass concentration measured by PPS and TEOM as a function of the median diameter (right).

The raw PPS measurement becomes reliable for soot generated with an oxidation air flowrate in the limited range of 1.3 to 1.5 L/min, where the mass concentration ratio between the PPS and the TEOM reference method remains nearly constant and close to 1, regardless of the measured median diameter. The mass concentration $C_{m,PPS\ raw}$ results have been corrected using Eq. (3) (Pandis et al., 1991):

$$C_{m,PPS\ corrected} = C_{m,PPS\ raw} \cdot \left(\frac{d_{s,Fuchs}}{d_0}\right)^{x(d_P)} \quad (3)$$

With $d_{S,\ Fuchs}$ the diameter of Fuchs active surface, evaluated from the size distribution for each measurement points ($d_{S,\ Fuchs}$ evaluated values are reported in table 2), $x(d_p)$ = 1.39 in the transition regime (30 nm to 150 nm) (Jung and Kittelson, 2005), and d_0 a reference diameter taken arbitrarily equal to 100 nm.

We also calculated the mass concentration based on the number size distribution measured by the SMPS. For this evaluation, we initially considered a constant so-called "true density", independent of the particle mobility diameter, but varying with the OC/TC ratio and therefore dependent on the selected operating point of the miniCAST. Indeed, as reported by several studies (Ouf et al., 2019; Park et al., 2004), the density of combustion soot particles decreases when the organic fraction increases, from the value of the elemental carbon density ρ_{EC} (close to 2000 kg.m^{-3}), down to the value of the organic carbon density ρ_{OC}. For diesel soot particles, Park et al. (2004) proposed to evaluate the true aggregate density through a mixing law based on the mass fraction of organic carbon (x=M_{OC} / (M_{OC}+ M_{EC})), ρ_{EC} and ρ_{OC} the respective density of elemental and organic carbon, and expressed as:

$$\rho_{true} = \frac{1}{\frac{x}{\rho_{OC}} + \frac{1-x}{\rho_{EC}}} \quad (4)$$

Based on data from a wide range of liquid, gaseous or solid fuel combustion soot, (Ouf et al., 2019) suggested that a constant true density could be considered with a mean value of ρ_{EC} =1834 kg.m^{-3} for soot with OC contents below 5%. In the absence of metallic compounds which is the case for the Mini-CAST soot, they also proposed considering three different ranges of the true density, as a function of x, the organic carbon to total carbon ratio: For low OC contents (i.e. below 5%) and high OC contents (i.e. above 20%), they consider respective constant true density values ρ_{EC} and ρ_{OC}. For intermediate OC content values between these two reference points, a linear mixing law as a function of *x* is suggested by (Ouf et al., 2019). Using this zone-based approach, we observed an underestimation of soot mass for almost all measurement points. Therefore, we considered using the Park mixing model (Eq. 4), with the values ρ_{EC} =1834 kg.m^{-3} for x=0, and ρ_{OC} = 1285 kg.m^{-3}, as suggested by (Ouf et al., 2019). We report in table 2 the values obtained for the OC/TC ratios as determined by thermo-optical analysis and the corresponding true densities calculated with the Park mixing model (Eq. 4) that were used to evaluate the "SMPS true density" mass concentrations reported on Fig. 8. The measured values of the OC/TC organic fraction contained in soot compare well with those obtained in the previous study by (Marhaba et al., 2019) for equivalent operating conditions of the Mini-CAST. For the considered points named CAST1, CAST2 and CAST3 in Marhaba et al. study (CAST3 corresponds to 1 L/min, CAST2 to 1.15 L/min and CAST1 to 1.5 L/min of oxidation airflow), Marhaba et al. reported OC/TC ratio values of 87%, 46.8% and 4.1%, respectively. In the same operating conditions, we measured corresponding OC/TC values of respectively 56.7%, 46% and 6.2%. For the point CAST3, our measured value is significantly lower, while the two other points are coherent. However, as highlighted by (Moore et al., 2014), soot production conditions can vary with parameters other than the overall carbon/oxygen ratio of the flame, and variations in mode size or OC/TC ratio have already been observed between different studies using different Cast or Mini-CAST generators. This makes it difficult to directly compare OC/TC data between studies conducted with this type of generator and justify the necessity to carry out the thermo-optical analysis of the organic content of the soot.

Table 2 – Properties, true density and effective density $\rho_{eff,100}$ of considered emitted soot particles

Oxidation air (L.min^{-1})	OC/TC	$d_{s,Fuchs}$ (nm)	True density (kg.m^{-3}), calculated with Equ. 4	$\rho_{eff,100}$ (kg.m^{-3}) calculated with Equ. 6
0.9	68.2%	28	1420	1382
1	56.7%	42	1476	1306
1.15	46.0%	62	1533	1235
1.2	43.3%	71	1548	1217
1.25	37.7%	83	1580	1180
1.3	24.3%	97	1662	1092
1.35	22.7%	110	1672	1081
1.5	6.2%	113	1787	972

As can be observed on Fig. 8, for the mass concentrations determined from SMPS size distributions and the true density, as well as for the evaluations based on the corrected PPS, we observe good agreement with the mass concentration obtained from the TEOM : except for a very limited number of points and at very low mass concentration measurements, both mass concentrations evaluated from the "SMPS, true density" and by the PPS after correction fall within a 10% interval of the TEOM reference mass concentration.

Furthermore, other approaches have been developed to estimate an "effective density" of soot particles, considering their fractal nature. These methods are based on so-called tandem techniques (Ghazi et al., 2013; Maricq and Xu, 2004; Tavakoli and Olfert, 2014) for evaluating this effective density. Based on an analysis of various data sets available in the literature, Olfert and Rogak (2019) proposed a model that expresses the effective density as a function of the mobility diameter:

$$\rho_{eff} = \rho_{eff,100}\left(\frac{d_m}{100}\right)^{-0.52} \text{ and with } m = \rho_{eff} \cdot \pi d_m^3/6 \quad (5)$$

with d_m the aggregate mobility diameter, m its mass, and $\rho_{eff,100}$ the effective density for aggregates with a 100 nm reference scale. This model allows the evaluation of the decrease in effective density with the mobility diameter d_m of soot aggregates. The data used to develop this model originates primarily from studies of particles produced by internal combustion engines or gas turbines, and a value of 510 kg.m^{-3} for the effective density at 100 nm was proposed by Olfert and Rogak. However, Yon et al. (2015) reported higher effective density values at 100 nm for the miniCAST, with values ranging from 1100 to 765 kg/m³ for oxidation air flow rates between 1 and 1.5 L/min. Although only three operating points were investigated, the decrease in effective density with increasing oxidation air flow rate was found to be linear. And we observed that the decay in OC/TC with oxidation air flowrate is also linear. We therefore conducted a 'best fit' identification procedure to obtain the values of $\rho_{eff,100}$, the density at 100 nm that would allow us to recover the TEOM reference mass concentrations from the SMPS analysis together with the Olfert and Rogak model. We obtained a set of values $\rho_{eff,100}$ "Best fit analysis" (see Fig. 7) and observed that the change in this density at 100 nm with the OC/TC ratio that can be represented by a linear interpolation, expressed as:

$$\rho_{eff,100}(x) = 932 + 661 \cdot x \quad (6)$$

with x the OC/TC ratio.

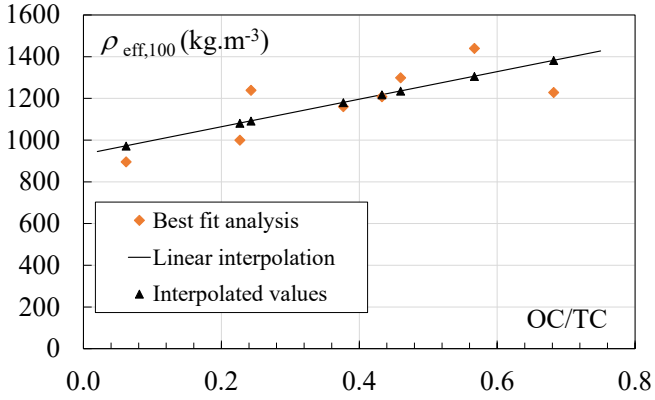

Figure 7 – Identification of $\rho_{eff,100}$ as a function of OC/TC ratio.

From the Equ. (6), interpolated values of $\rho_{eff,100}$ can be evaluated. These effective densities at 100 nm determined through this procedure are reported in Table 2, and the corresponding mass concentrations, labeled "SMPS effective density," are shown in Fig. 8: the use of this effective density model combined with the measured size distributions results in a good estimation of the mass concentration.

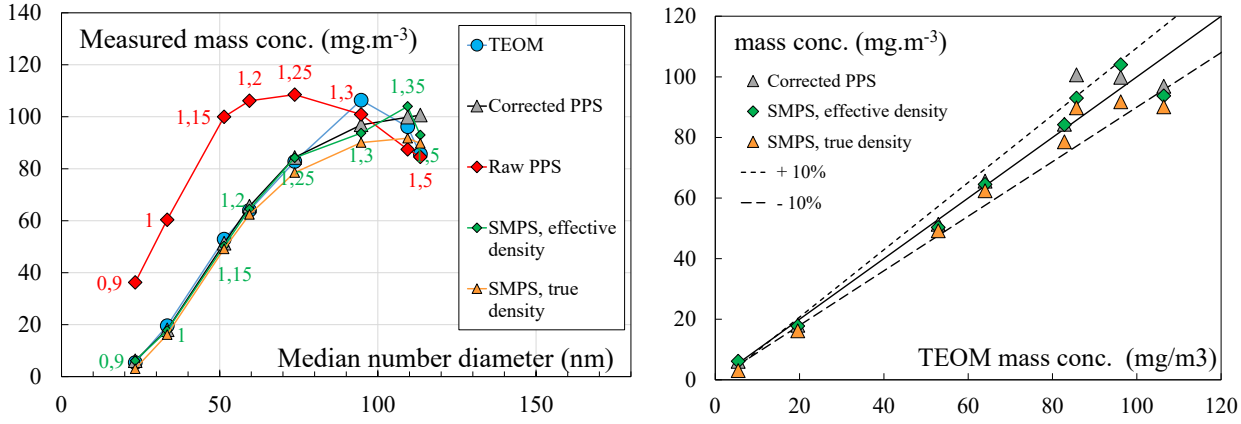

Figure 8 – Comparison of TEOM mass concentrations with evaluations based on PPS and SMPS measurements.

Fig. 9 shows the mass concentrations measured by the MA300 for ultraviolet and infrared wavelengths, as a function of those measured by the TEOM reference method for soot produced with the different oxidation air flow rates tested (value indicated next to each measuring point, in L.min^{-1}). For oxidation air of 0.9 L.min^{-1}, the soot generated is 68% composed by organic carbon. This percentage drops to around 6% for those generated with 1.5 L.min^{-1} oxidation air.

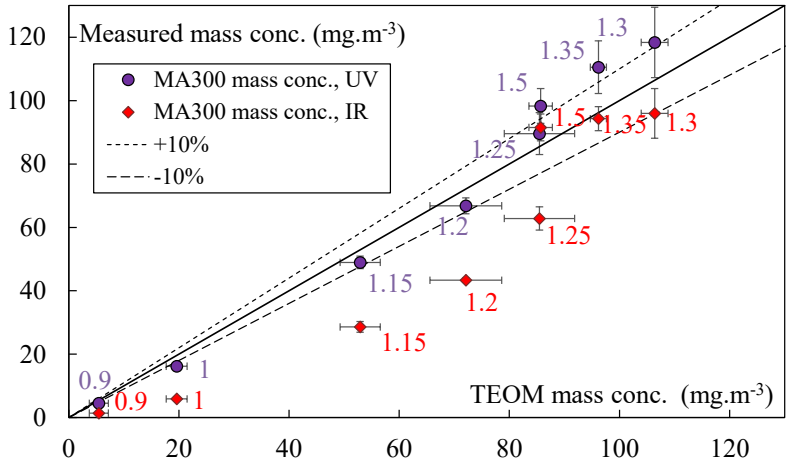

Figure 9 – Mass concentrations measured by the MA300 as a function of the TEOM reference measurements

The MA300 measurement becomes reliable at infrared wavelengths for soot generated with an oxidation air flow rate of between 1.3 L/min and 1.5 L/min, which are soot particles predominantly made up of elemental carbon (less than 24% of OC). For ultraviolet wavelengths, measurements are reliable for soot generated with oxidation airflows of less than 1.3 L/min, and therefore with high organic carbon ratios, at least higher than 38%.

Conclusion

For this intercomparison of instruments and measurement techniques for the evaluation of the soot mass concentration, we used a Mini-CAST generator commonly employed in laboratory experiments to produce soot particles under stable and controlled conditions. This generator allows to generate soot representative of that emitted by internal combustion engines, as well as in fire situations or during biomass combustion. By significantly and continuously varying one of the Mini-CAST parameters, we were able to generate a set of eight soot particles measurement points, with significant variations in the organic to total carbon ratio OC/TC, ranging from 6% to 68%, as well as in their size distributions, while also achieving mass concentrations covering values from 7 to 96 $mg \cdot m^{-3}$. Over almost two decades of mass concentration range, we obtained a very good correlation between the gravimetric method using filter sampling, the real-time online methods with the reference TEOM instrument, and the offline thermo-optical analysis, which also provided access to the OC/TC fraction. Based on the electrical charging of the aerosol particles, the Pegasor Particle Sensor (PPS) analyser provides a real-time measurement of the mass concentration at one Hertz frequency, but with a response that depends on the particle size distribution. We established that with an appropriate correction based on the aerosol active surface, it can also provide relevant quantitative information on the soot mass concentration. Finally, the MA300 aethalometer was evaluated over a wide range of OC/TC ratios. In this instrument, the measurement technique is based on the attenuation of a light beam with different wavelength through a particle cake accumulating on a filter. This attenuation is dependent on the wavelength, and on the OC/TC ratio. We were able to

determine a limit in soot organic content, with a maximum value of OC/TC=24% for which the infrared measurement allows quantification of the total mass concentration, rather than only the so-called "black carbon" fraction. We also established that the ultraviolet wavelength usually used to quantify brown carbon can also provide an evaluation of the total mass concentration, when the organic carbon ratios is sufficiently high, at least higher than 38%. For the analysis of soot mass concentration based on SMPS size distribution measurements, we applied two methods: one based on a "true density," constant for each operating point of the miniCAST, and a second one that accounts for the effective density of the aggregates, considering both their mobility diameter and the OC/TC ratio. Originally, in the considered model of Olfert and Rogak (2019), the effective density of aggregates is calculated based on their mobility diameter and on a constant reference effective density at 100 nm. In this work, we propose to consider that this reference effective density is a function of the OC/TC ratio. This approach considering both the OC/TC ratio and the mobility diameter results in mass concentrations in good agreement with the reference TEOM measurements. The results of this study show that the selected operating points led to simultaneous variations in mass concentration, size distribution, and OC/TC ratio. It would be relevant, by varying other gas flow rates of the miniCAST or the aerosol dilution conditions, to better decouple the parameters under investigation in future studies.

Authors contribution:

BS and AK planned the measurement campaign; BS, AK and GP performed the measurements; BS, AK and GP analysed the data; BS and AK wrote the manuscript draft; BS and AK reviewed and edited the manuscript.

Competing interests:

The authors declare that they have no conflict of interest.

Data availability:

The raw data can be provided upon request to the authors.

References

Aakko-Saksa, P., Kuittinen, N., Murtonen, T., Koponen, P., Aurela, M., Järvinen, A., Teinilä, K., Saarikoski, S., Barreira, L.M.F., Salo, L., Karjalainen, P., Ortega, I.K., Delhaye, D., Lehtoranta, K., Vesala, H., Jalava, P., Rönkkö, T., Timonen, H., 2022. Suitability of different methods for measuring black carbon emissions from marine engines. Atmosphere (Basel) 13. https://doi.org/10.3390/atmos13010031

Allen, G., Sioutas, C., Koutrakis, P., Reiss, R., Lurmann, F.W., Roberts, P.T., 1997. Evaluation of the TEOM® Method for Measurement of Ambient Particulate Mass in Urban Areas. J Air Waste Manage Assoc 47, 682–689. https://doi.org/10.1080/10473289.1997.10463923

Bescond, A., Yon, J., Ouf, F.X., Rozé, C., Coppalle, A., Parent, P., Ferry, D., Laffon, C., 2016. Soot optical properties determined by analyzing extinction spectra in the visible near-UV: Toward an optical speciation according to constituents and structure. J Aerosol Sci 101, 118–132. https://doi.org/10.1016/j.jaerosci.2016.08.001

Blanco-Donado, E.P., Schneider, I.L., Artaxo, P., Lozano-Osorio, J., Portz, L., Oliveira, M.L.S., 2022. Source identification and global implications of black carbon. Geoscience Frontiers 13, 101149. https://doi.org/10.1016/J.GSF.2021.101149

Chakraborty, M., Giang, A., Zimmerman, N., 2023. Performance evaluation of portable dual-spot micro-aethalometers for source identification of black carbon aerosols: Application to wildfire smoke and traffic emissions in the Pacific Northwest. Atmos Meas Tech 16, 2333–2352. https://doi.org/10.5194/amt-16-2333-2023

Chow, J.C., Watson, J.G., Crow, D., Lowenthal, D.H., Merrifield, T., 2001. Comparison of IMPROVE and NIOSH Carbon Measurements. Aerosol Science and Technology 34, 23–34. https://doi.org/10.1080/02786820119073

Collaud Coen, M., Weingartner, E., Apituley, A., Ceburnis, D., Fierz-Schmidhauser, R., Flentje, H., Henzing, J.S., Jennings, S.G., Moerman, M., Petzold, A., Schmid, O., Baltensperger, U., 2010. Minimizing light absorption measurement artifacts of the Aethalometer: evaluation of five correction algorithms. Atmos Meas Tech 3, 457–474. https://doi.org/10.5194/amt-3-457-2010

Drinovec, L., Močnik, G., Zotter, P., Prévôt, A.S.H., Ruckstuhl, C., Coz, E., Rupakheti, M., Sciare, J., Müller, T., Wiedensohler, A., Hansen, A.D.A., 2015. The "dual-spot" Aethalometer: An improved measurement of aerosol black carbon with real-time loading compensation. Atmos Meas Tech 8, 1965–1979. https://doi.org/10.5194/amt-8-1965-2015

Elomaa, J.T., Luoma, K., Harni, S.D., Virkkula, A., Timonen, H., Petäjä, T., 2025. The applicability and challenges of black carbon sensors in monitoring networks. Aerosol Research 3, 293–314. https://doi.org/10.5194/ar-3-293-2025

Favez, O., Cachier, H., Sciare, J., Le Moullec, Y., 2007. Characterization and contribution to PM2.5 of semi-volatile aerosols in Paris (France). Atmos Environ 41, 7969–7976. https://doi.org/10.1016/j.atmosenv.2007.09.031

Ghazi, R., Tjong, H., Soewono, A., Rogak, S.N., Olfert, J.S., 2013. Mass, mobility, volatility, and morphology of soot particles generated by a mckenna and inverted burner. Aerosol Science and Technology 47, 395–405. https://doi.org/10.1080/02786826.2012.755259

Gren, L., Krais, A.M., Assarsson, E., Broberg, K., Engfeldt, M., Lindh, C., Strandberg, B., Pagels, J., Hedmer, M., 2022. Underground emissions and miners' personal exposure to diesel and renewable diesel exhaust in a Swedish iron ore mine. Int Arch Occup Environ Health 95, 1369–1388. https://doi.org/10.1007/s00420-022-01843-x

Gundel, L.A., Dod, R.L., Rosen, H., Novakov, T., 1984. The relationship between optical attenuation and black carbon concentration for ambient and source particles. Science of The Total Environment 36, 197–202. https://doi.org/10.1016/0048-9697(84)90266-3

Hansen, A.D.A., Rosen, H., Novakov, T., 1984. The aethalometer — An instrument for the real-time measurement of optical absorption by aerosol particles. Science of The Total Environment 36, 191–196. https://doi.org/10.1016/0048-9697(84)90265-1

Jung, H., Kittelson, D.B., 2005. Characterization of aerosol surface instruments in transition regime. Aerosol Science and Technology 39, 902–911. https://doi.org/10.1080/02786820500295701

Kort, A., Ouf, F.X., Gelain, T., Malet, J., Lakhmi, R., Breuil, P., Viricelle, J.P., 2021. Quantification of soot deposit on a resistive sensor: Proposal of an experimental calibration protocol. J Aerosol Sci 156. https://doi.org/10.1016/j.jaerosci.2021.105783

Marhaba, I., Ferry, D., Laffon, C., Regier, T.Z., Ouf, F.X., Parent, P., 2019. Aircraft and MiniCAST soot at the nanoscale. Combust Flame 204, 278–289. https://doi.org/10.1016/j.combustflame.2019.03.018

Maricq, M.M., 2013. Monitoring Motor vehicle pm emissions: An evaluation of three portable low-cost aerosol instruments. Aerosol Science and Technology 47, 564–573. https://doi.org/10.1080/02786826.2013.773394

Maricq, M.M., Xu, N., 2004. The effective density and fractal dimension of soot particles from premixed flames and motor vehicle exhaust. J Aerosol Sci 35, 1251–1274. https://doi.org/10.1016/j.jaerosci.2004.05.002

Mendoza, D.L., Hill, L.D., Blair, J., Crosman, E.T., 2024. A Long-Term Comparison between the AethLabs MA350 and Aerosol Magee Scientific AE33 Black Carbon Monitors in the Greater Salt Lake City Metropolitan Area. Sensors 24. https://doi.org/10.3390/s24030965

Moore, R.H., Ziemba, L.D., Dutcher, D., Beyersdorf, A.J., Chan, K., Crumeyrolle, S., Raymond, T.M., Thornhill, K.L., Winstead, E.L., Anderson, B.E., 2014. Mapping the operation of the miniature combustion aerosol standard (Mini-CAST) soot generator. Aerosol Science and Technology 48, 467–479. https://doi.org/10.1080/02786826.2014.890694

Ntziachristos, L., Amanatidis, S., Samaras, Z., Janka, K., Tikkanen, J., 2013. Application of the Pegasor Particle Sensor for the Measurement of Mass and Particle Number Emissions. SAE Int J Fuels Lubr 6, 521–531. https://doi.org/10.4271/2013-01-1561

Ntziachristos, L., Giechaskiel, B., Ristimäki, J., Keskinen, J., 2004. Use of a corona charger for the characterisation of automotive exhaust aerosol. J Aerosol Sci 35, 943–963. https://doi.org/10.1016/j.jaerosci.2004.02.005

Olfert, J., Rogak, S., 2019. Universal relations between soot effective density and primary particle size for common combustion sources. Aerosol Science and Technology. https://doi.org/10.1080/02786826.2019.1577949

Ouf, F.X., Bourrous, S., Fauvel, S., Kort, A., Lintis, L., Nuvoli, J., Yon, J., 2019. True density of combustion emitted particles: A comparison of results highlighting the influence of the organic contents. J Aerosol Sci 134, 1–13. https://doi.org/10.1016/j.jaerosci.2019.04.007

Ouf, F.X., Parent, P., Laffon, C., Marhaba, I., Ferry, D., Marcillaud, B., Antonsson, E., Benkoula, S., Liu, X.J., Nicolas, C., Robert, E., Patanen, M., Barreda, F.A., Sublemontier, O., Coppalle, A., Yon, J., Miserque, F., Mostefaoui, T., Regier, T.Z., Mitchell, J.B.A., Miron, C., 2016. First in-flight synchrotron X-ray absorption and photoemission study of carbon soot nanoparticles. Sci Rep 6. https://doi.org/10.1038/srep36495

Pandis, S.N., Baltensperger, U., Wolfenbarger, J.K., Seinfeld, J.H., 1991. Inversion of aerosol data from the epiphaniometer. J Aerosol Sci 22, 417–428. https://doi.org/10.1016/0021-8502(91)90002-Y

Park, K., Kittelson, D.B., McMurry, P.H., 2004. Structural properties of diesel exhaust particles measured by Transmission Electron Microscopy (TEM): Relationships to particle mass and mobility. Aerosol Science and Technology 38, 881–889. https://doi.org/10.1080/027868290505189

Rostedt, A., Arffman, A., Janka, K., Yli-Ojanperä, J., Keskinen, J., 2014. Characterization and response model of the PPS-M aerosol sensor. Aerosol Science and Technology 48, 1022–1030. https://doi.org/10.1080/02786826.2014.951023

Sipkens, T.A., Corbin, J.C., Chen, K., Rivellini, L.-H., Abbatt, J., Olfert, J.S., 2025. Quantitative uncertainty and post-processing for micro-aethalometers measuring black carbon. https://doi.org/10.5194/egusphere-2025-4209

Tavakoli, F., Olfert, J.S., 2014. Determination of particle mass, effective density, mass-mobility exponent, and dynamic shape factor using an aerodynamic aerosol classifier and a differential mobility analyzer in tandem. J Aerosol Sci 75, 35–42. https://doi.org/10.1016/j.jaerosci.2014.04.010

Virkkula, A., Mäkelä, T., Hillamo, R., Yli-Tuomi, T., Hirsikko, A., Hämeri, K., Koponen, I.K., 2007. A simple procedure for correcting loading effects of aethalometer data. J Air Waste Manage Assoc 57, 1214–1222. https://doi.org/10.3155/1047-3289.57.10.1214

Weingartner, E., Saathoff, H., Schnaiter, M., Streit, N., Bitnar, B., Baltensperger, U., 2003. Absorption of light by soot particles: Determination of the absorption coefficient by means of aethalometers. J Aerosol Sci 34, 1445–1463. https://doi.org/10.1016/S0021-8502(03)00359-8

Wu, L., Shen, Y., Che, F., Zhang, Y., Gao, J., Wang, C., 2024. Evaluating the performance and influencing factors of three portable black carbon monitors for field measurement. J Environ Sci (China) 139, 320–333. https://doi.org/10.1016/j.jes.2023.05.044

Yon, J., Bescond, A., Ouf, F.X., 2015. A simple semi-empirical model for effective density measurements of fractal aggregates. J Aerosol Sci 87, 28–37. https://doi.org/10.1016/j.jaerosci.2015.05.003